2008

Immunohistochemical assessment of cyclic guanosine monophosphate (cGMP) and soluble guanylate cyclase (sGC) within the rostral ventrolateral medulla

Kellysan Powers-Martin
Murdoch University

Anna M. Barron
Murdoch University

Clare H. Auckland
Murdoch University

John K. Mccooke
Murdoch University

Douglas J. McKitrick
University of Western Australia

See next page for additional authors

Immunohistochemical assessment of cyclic guanosine monophosphate (cGMP) and soluble guanylate cyclase (sGC) within the rostral ventrolateral medulla

Abstract

Functional evidence suggests that nitric oxide (NO) signalling in the rostral ventrolateral medulla (RVLM) is cGMP-dependent and that this pathway is impaired in hypertension. We examined cGMP expression as a marker of active NO signalling in the C1 region of the RVLM, comparing adult (>18 weeks) Wistar-Kyoto (WKY, n = 4) and spontaneously hypertensive rats (SHR, n = 4). Double label immunohistochemistry for cGMP-immunoreactivity (IR) and C1 neurons [as identified by phenylethanolamine N-methyltransferase (PNMT-IR) or tyrosine hydroxylase TH-IR)], or neuronal NO synthase (nNOS) neurones, failed to reveal cGMP-IR neurons in the RVLM of either strain, despite consistent detection of cGMP-IR in the nucleus ambiguus (NA). This was unchanged in the presence of isobutylmethylxanthine (IBMX; 0.5 mM, WKY, n = 4, SHR n = 2) and in young animals (WKY, 10-weeks, n = 3). Incubation of RVLM-slices (WKY, 10-weeks, n = 9) in DETA-NO (100 μm; 10 min) or NMDA (10 μM; 2 min) did not uncover cGMP-IR. In all studies, cGMP was prominent within the vasculature. Soluble guanylate cyclase (sGC)-IR was found throughout neurones of the RVLM, but did not co-localise with PNMT, TH or nNOS-IR neurons (WKY, 10-weeks, n = 6). Results indicate that within the RVLM, cGMP is not detectable using immunohistochemistry in the basal state and cannot be elicited by phosphodiesterase inhibition, NMDA receptor stimulation or NO donor application.

Authors

Kellysan Powers-Martin, Anna M. Barron, Clare H. Auckland, John K. Mccooke, Douglas J. McKitrick, Leonard F. Arnolda, and Jacqueline K. Phillips

ORIGINAL PAPER

Immunohistochemical assessment of cyclic guanosine monophosphate (cGMP) and soluble guanylate cyclase (sGC) within the rostral ventrolateral medulla

Kellysan Powers-Martin · Anna M. Barron · Clare H. Auckland ·
John K. McCooke · Douglas J. McKitrick · Leonard F. Arnolda ·
Jacqueline K. Phillips

Abstract Functional evidence suggests that nitric oxide (NO) signalling in the rostral ventrolateral medulla (RVLM) is cGMP-dependent and that this pathway is impaired in hypertension. We examined cGMP expression as a marker of active NO signalling in the C1 region of the RVLM, comparing adult (>18 weeks) Wistar–Kyoto (WKY, $n = 4$) and spontaneously hypertensive rats (SHR, $n = 4$). Double label immunohistochemistry for cGMP-immunoreactivity (IR) and C1 neurons [as identified by phenylethanolamine N-methyltransferase (PNMT-IR) or tyrosine hydroxylase TH-IR)], or neuronal NO synthase (nNOS) neurones, failed to reveal cGMP-IR neurons in the RVLM of either strain, despite consistent detection of cGMP-IR in the nucleus ambiguus (NA). This was unchanged in the presence of isobutylmethylxanthine (IBMX; 0.5 mM, WKY, $n = 4$, SHR $n = 2$) and in young animals (WKY, 10-weeks, $n = 3$). Incubation of RVLM-slices (WKY, 10-weeks, $n = 9$) in DETA-NO (100 μm; 10 min) or NMDA (10 μM; 2 min) did not uncover cGMP-IR. In all studies, cGMP was prominent within the vasculature. Soluble guanylate cyclase (sGC)-IR was found throughout neurones of the RVLM, but did not co-localise with PNMT, TH or nNOS-IR neurons (WKY, 10-weeks, $n = 6$). Results indicate that within the RVLM, cGMP is not detectable using immunohistochemistry in the basal state and cannot be elicited by phosphodiesterase inhibition, NMDA receptor stimulation or NO donor application.

Kellysan Powers-Martin and Anna M. Barron contributed equally.

K. Powers-Martin · A. M. Barron · C. H. Auckland · J. K. McCooke · J. K. Phillips (✉)
Division of Health Sciences, School of Veterinary and Biomedical Science, Murdoch University, South St. Murdoch, Perth, WA 6150, Australia
e-mail: j.k.phillips@murdoch.edu.au

C. H. Auckland · J. K. Phillips
State Agricultural Biotechnology Centre, Murdoch, Perth, WA 6150, Australia

D. J. McKitrick · L. F. Arnolda
Cardiology Research, Royal Perth Hospital, School of Medicine and Pharmacology, The University of Western Australia, Perth, WA, Australia

Introduction

The rostral ventrolateral medulla (RVLM) contributes significant excitatory drive to sympathetic preganglionic neurons and therefore also to vascular tone via two well characterised subpopulations of bulbospinal neurons: the C1 (adrenergic) and non-C1 cell groups [1–3]. Glutamate is the major neurotransmitter driving the activity of these neurons [3, 4], but the gaseous neurotransmitter nitric oxide (NO) is thought to play a key role in regulating glutamate induced pressor responses, and therefore modulating homeostatic blood pressure mechanisms [5–7]. Altered NO signalling in the RVLM is associated with increased sympathetic outflow in animal models of hypertension [8], however the mechanism of action is unclear, with a range of effects consistent with NO-mediated pressor, depressor or neutral effects being reported [9–11].

One of the most widely studied and best-understood NO second messenger systems is the activation of soluble guanylate cyclase (sGC) and the subsequent generation of intracellular $3',5'$-cyclic guanosine monophosphate (cGMP) [12, 13]. Soluble GC is a heme-containing

heterodimer of α and β subunits, with the β1 subunit being the major subunit, as there is no catalytic activity in its' absence [14, 15]. Activation of NMDA receptors can drive this pathway, with increased intracellular Ca^{2+} stimulating the Ca^{2+}/calmodulin NO system, promoting conversion of L-Arginine to NO. Intracellular cGMP levels can also be regulated by membrane bound, or particulate guanylyl cyclases, incorporating the receptors for atrial (ANP), brain (BNP) and C-type (CNP) natriuretic peptides [13]. As a second messenger, cGMP can target various protein kinases and ion channels, and its activity is limited through degradation by phosphodiesterases (PDE) [13].

Nitric oxide has alternative neuromodulatory mechanisms. This includes the *S*-nitrosylation of proteins and in particular that of NMDA receptors [12], and interactions with superoxide, with the resultant peroxynitrite having potent oxidising properties that convey a variety of physiological and pathophysiological effects [16].

Within the RVLM, all three NO synthase (NOS) isoforms are present [17] and we have shown recently that neuronal (n)NOS is increased in the RVLM of spontaneously hypertensive rats (SHR) [18]. Work by Chan et al. [19] suggests that the relative balance of functional nNOS versus inducible (i)NOS activity determines RVLM output, and further, that the different NOS isoforms activate different downstream signals, with nNOS driving sGC/cGMP-dependent sympathoexcitatory responses, and NO produced by iNOS driving peroxynitrite formation and sympathoinhibitory responses [20]. Glutamate-induced pressor responses in the RVLM are in general proposed to be modulated by NO-sGC/cGMP [5, 6, 21] and this is supported by electrophysiological studies showing cGMP-dependent potentiation of glutamate currents in RVLM slice preparations [7].

To date, no studies have described the immunohistochemical localisation of neurons capable of expressing cGMP within the C1 region [22]. Given the strong evidence that NO signalling plays a functional role in the RVLM, we sought to identify the cellular targets for NO in the RVLM, visualising cGMP and its neuroanatomical relationship with the C1 cell group, as identified by the presence of tyrosine hydroxylase (TH) or phenylethanolamine *N*-methyltransferase (PNMT), and the more medially located nNOS expressing cell population [18, 23]. Given that studies in SHR show augmented pressor responses to microinjection of glutamate in the RVLM [24, 25], we considered the hypothesis that the NO downstream signalling sGC/cGMP pathway may be altered. We therefore also sought to examine if altered cGMP expression, as determined using fluorescence immunohistochemistry, was demonstrable in the RVLM of the SHR when compared its genetic control, the Wistar Kyoto (WKY). An inability to detect cGMP-immunoreactivity (-IR) in the RVLM of

either strain led to additional studies that sought to increase synthesis of cGMP in fresh RVLM brain slices, and examine sGC-IR throughout the region.

Materials and methods

Animals

Animals were obtained from the Animal Resources Centre, Murdoch, Western Australia and all procedures conformed to the guidelines approved by the Murdoch University Animal Ethics Committee. Rats were housed on a 12 h light-dark cycle with access to standard rat chow and water ad libitum. Male rats were used in all experiments. Wistar–Kyoto ($n = 26$ in total) and SHR ($n = 8$ total) animals were used in the different age groups as detailed in each experimental protocol.

Animal tissue preparation for immunohistochemistry

Rats were anaesthetised with sodium pentobarbitone (Thiobarb, Jurox, Rutherford, Australia; 100 mg/kg) administered intraperitoneally. A pre-fixation solution of ice-cold heparinised saline (30 ml, 0.9% NaCl containing 2,000 I.U. of heparin [Jurox, Rutherford, Australia]) was perfused via the ascending aorta (6 ml per minute), followed by 180 ml of ice-cold 3.7% formalin diluted in 0.9% saline at the same rate. In one set of experiments, the phosphodiesterase inhibitor isobutylmethylxanthine (IBMX; 0.5 mM Sigma, St. Louis, MO) was added to the pre-fixation saline solution. Brains were removed and post fixed in 4% formalin for 4 h at 4°C. Tissue was washed in 0.1 M phosphate buffered saline (PBS, pH 7.4) (3 × 10 min) and coronal hindbrain sections (50 μm) sections were cut using a vibrating microtome (Vibratome, St. Louis, MO). Sections were split into two alternate series, with each section therefore 100 μm apart. Sections were then incubated in 50% ethanol for 30 min and then washed in 0.01 M PBS containing 10 mM Tris (TPBS; 2 × 15 min).

Animal tissue preparation for brainstem slice in-vitro incubation

Animals were anaesthetised and perfused as for the immunohistochemical experiments. Perfusate consisted of ice-cold sucrose based cutting solution (2 mM KCl, 2 mM $MgSO_4$, 1.25 mM NaH_2PO_4, 1 mM $MgCl_2$, 26 mM $NaHCO_3$, 0.1 mM $CaCl_2$, 10 mM D-glucose, 248 mM sucrose, 95% O_2/5% CO_2, pH 7.4 [26] containing IBMX (0.5 mM) and heparin 1,000 U/ml (Jurox). The brains were removed immediately and coronal RVLM sections (400 μm) were cut on a vibrating

microtome while immersed in the same ice-cold sucrose cutting solution.

After cutting, brain slices were warmed to 37°C over 20 min in an artificial cerebrospinal fluid (aCSF) solution (124 mM NaCl, 2 mM KCl, 2 mM MgSO$_4 \cdot$ 7H$_2$O, 1.25 mM NaH$_2$PO$_4$, 26 mM NaHCO$_3$, 2 mM CaCl$_2$, 10 mM D-glucose, 0.5 mM IBMX, 95% O$_2$/5% CO$_2$, pH 7.4) [26]. Once at 37°C, slices were incubated for a further 30 min, prior to incubation in either 100 μM NMDA (Sigma) plus 10 μM glycine for 1 × 5 min [27] or 100 μM DETA-NO (Sigma) for 1 × 15 min [28] in aCSF solution. Twenty minutes prior to use, DETA-NO was prepared in aCSF buffer and warmed to 37°C to stabilise NO release. Submerging the slices in ice-cold 3.7% formalin terminated the reaction. Control slices were incubated in aCSF solution only. Slices were post-fixed for 2 h in 3.7% formalin at 4°C, followed by washing in 0.1 M PBS (1 × 30 min). Slices were then cryoprotected in 30% sucrose in 0.1 M PBS and sodium azide (NaN$_3$, 0.1%; overnight) prior to cutting 50 μm sections on a cryostat (Leica CM1510; Leica Microsystems GmbH, Wetzlar, Germany) at −17°C for subsequent immunohistochemistry using alternate sections as described above.

Immunohistochemistry

Sections were pre-treated for one hour at room temperature in blocking solution containing 10% donkey serum (Chemicon, Temecula, CA), diluted in TPBS with 0.3% Triton-X (Tx) and 0.1% NaN$_3$. They were then incubated free floating in different combinations of primary antibody [cGMP/nNOS, cGMP/PNMT or TH, sGC/nNOS, sGC/PNMT, sGC/Protein Gene Product (PGP9.5) or sGC/glial fibrillary acidic protein (GFAP)] at pre-optimised concentrations (Table 1) for 24 h at room temperature, then 72–96 h at 4°C. From each animal, the RVLM was split into two series of alternating sections, allowing two different antibody combinations per animal. Antibodies were diluted in blocking solution. Sections were then washed (3 × 30 min TPBS) and incubated with species specific secondary antibodies (Table 1) for 12–14 h at 4°C, diluted in TPBS with 0.3% Tx, 0.1% NaN$_3$ and 1% donkey serum. Finally, sections were washed (3 × 30 min TPBS), mounted on slides and cover slipped with ProLong Antifade (Molecular Probes, Eugene, OR USA).

The RVLM region examined was defined as that area extending caudally 600–800 μm from the caudal pole of the facial nucleus. This corresponds to −12.5 to −11.7 mm from Bregma [29] bounded laterally by the spinal trigeminal tract, medially by the inferior olive and pyramids, and dorsally by the compact formation of the NA. Sections were arranged in a rostro-caudal orientation prior to mounting and all sections were examined bilaterally for immunostaining. The NA from each series of sections was used as an internal control for cGMP-IR as it consistently demonstrated neuronal expression.

Control experiments

For negative controls, RVLM tissue sections were incubated in blocking solution alone (no antibody controls) and run in parallel to each of the experimental protocols.

Positive control experiments for the cGMP, sGC and PGP9.5 antibodies were performed using additional sections from animals used in the experiments described above. For sGC, sections of cerebellum were processed in parallel to RVLM sections. A TH/PGP9.5 double label combination was used as a positive control for the PGP9.5 antibody. To confirm that the cGMP antibody was detecting both neuronal and vascular elements, a cGMP/mouse anti alpha-smooth muscle actin (alpha-SMA) double label combination was used (Table 1).

Previous studies and manufacturers product information have documented the specificity of antibody reactions and/or characteristic staining patterns for the cGMP [30, 31], nNOS [32], sGC [33], PNMT [34], TH [35], PGP-9.5 [36, 37], GFAP [38] and SMA [39] antibodies.

Imaging and analysis

A BioRad MRC-1024 confocal laser-scanning microscope (Carl Zeiss Pty. Ltd. North Ryde, NSW, Australia) was used to examine immunofluorescence with filter settings for identification of secondary antibody fluorophores (fluorescein isothiocyanate [FITC], cyanine [CY2] and indocarbocyanine [CY3]). Each fluorochrome was viewed separately in single channel mode and no "bleed through" was observed. To excite FITC labelled and CY2 secondary antibodies, excitation was set at 488 nm, while 568 nm excitation was used for CY3. Images were captured by taking 4–6 optical "slices" through the sections as a "z" series imaging 10–30 microns of tissue, and then reconstructed as a single two-dimensional image using Confocal Assistant Software (BioRad). Figures were assembled and labelled using Photo Shop software (version 6, Adobe Systems, Mountain View, CA). Overall colour balance and contrast were adjusted, but no other modifications were made.

Results

Detection of cGMP-IR in the RVLM

Cells expressing either the adrenergic markers PNMT/TH, or nNOS, were used to delineate the neuronal populations

Table 1 Primary and secondary antibodies: dilutions and source

Antigen and host species	Dilution	Product code and source
Primary detection antibodies		
Anti cGMP: Rabbit polyclonal	1:500	AB303: Chemicon (Temecula CA, USA)
Anti nNOS: Mouse monoclonal	1:400	N2280: Sigma (St. Louis, MO, USA)
Anti PNMT: Sheep polyclonal	1:500	AB146: Chemicon
Anti TH: Mouse monoclonal	1:300	22941: Clone LNC1, Immunostar (Hudson, Wisconsin, USA)
Anti sGC (β1-subunit): Rabbit polyclonal	1:500	160897: Cayman Chemicals (Ann Arbour, MI USA)
Anti PGP9.5: Guinea pig polyclonal	1:750	AB5898: Chemicon
Anti GFAP: Mouse monoclonal	1:750	G3893, clone G-A 5: Sigma
Anti alpha-SMA: Mouse monoclonal	1:500	A5228, clone 1A4: Sigma
Secondary detection antibodies		
FITC: Donkey anti-mouse IgG	1:500	Jackson (West Grove, PA)
CY2: Donkey anti-sheep IgG	1:500	Jackson
CY3: Donkey anti-rabbit IgG	1:500	Jackson
CY3: Donkey anti-guinea pig IgG	1:750	Jackson
CY3: Donkey anti-mouse IgG	1:750	Jackson

Cyclic guanosine monophosphate (cGMP); neuronal nitric oxide synthase (nNOS), phenylethanolamine *N*-methyltransferase (PNMT), tyrosine hydroxylase (TH), soluble guanylate cyclase (sGC), Protein Gene Product-9.5 (PGP9.5), Glial fibrillary acidic protein (GFAP), alpha-Smooth Muscle Actin (alpha-SMA), fluorescein isothiocyanate (FITC), cyanine (CY2), indocarbocyanine (CY3)

of interest within the RVLM. PNMT/TH neurons defined the rostro-caudal axis of the C1 adrenergic cell group while nNOS cell bodies bounded the medial RVLM region [29]. In the first series of experiments, sections from mature WKY ($n = 4$) and SHR ($n = 4$) (>18 weeks) were examined for double labelling for cGMP/PNMT-IR and cGMP/nNOS-IR. Results showed very few cGMP immunoreactive neurons in the RVLM in association with either the C1 adrenergic or the nNOS cells groups in either strain of mature animal and no cells were double labelled for either cGMP:PNMT or cGMP:nNOS (Fig. 1a–f). There was strong cGMP-IR in the NA (Fig. 1b, f) and in these cells, staining was punctate in appearance, and localised to the cytoplasm and extending neurites. Cyclic GMP-IR was visible in the vasculature throughout the sections.

To control for rapid degradation of cGMP, in the second series of experiments, additional adult WKY ($n = 4$) and SHR ($n = 2$) were assessed after perfusion with IBMX (0.5 mM) in the pre-perfusate solution. Double labelling was performed for cGMP and either PNMT/TH or nNOS. The presence of IBMX did not reveal any increase in the number of cGMP-IR neurons in the RVLM and did not alter the PNMT, TH or nNOS-IR (data not shown). There was a visible increase in the intensity of staining for cGMP in cells of the NA and within blood vessels of the RVLM region in both the WKY and SHR (Fig. 2). To assess the influence of animal age, in the third series of experiments, immunohistochemistry for cGMP/PNMT was performed in young male WKY animals (10 weeks; $n = 3$). The pattern

of immunoreactivity was the same as that seen in the adult WKY, with very few cells outside of the NA showing cGMP-IR above the level of background in the RVLM region (data not shown).

Detection of cGMP-IR in brainstem slices after incubation in-vitro

In the fourth series of experiments, cGMP-IR in the RVLM was examined in brainstem slices that were treated in-vitro using experimental paradigms designed to increase cGMP synthesis. Due to the extended time frame of the experimental protocol, all experiments were performed in the presence of IBMX (0.5 mM). Sections were examined after incubation of brainstem slices in-vitro in aCSF (control), with 100 μM NMDA or the NO donor DETA-NO (100 μM; $n = 3$ for each experiment, total $n = 9$ WKY 10 week-old animals). In the aCSF control experiments, the location of neuronal cGMP staining was comparable with that from the fixation perfused experiments (Fig. 3a, b). However, tissue integrity and overall fluorescence was reduced in this series of experiments due to the incubation protocol and the requirement for cryoprotection prior to sectioning. In those brainstem slice preparations incubated with NMDA (Fig. 3c, d) or DETA-NO (Fig. 3e, f), the cGMP staining in the vasculature and NA was brighter when compared to control (aCSF) preparations (inset panels b′, d′ and f′), but no additional neuronal staining in RVLM neurons was uncovered (Fig. 3).

Fig. 1 Confocal images depicting double labelling for PNMT/cGMP (**a**, **b**) and nNOS/cGMP (**c**, **d**) in the RVLM of adult WKY in the absence of IBMX, and PNMT/cGMP (**e**, **f**) in the RVLM of an adult SHR in the absence of IBMX. PNMT-immunoreactivity (**a**, **e**) indicates the location of the C1 adrenergic cell group. Panel (**c**) illustrates nNOS immunoreactive cells, located adjacent to the inferior olive (IO) in the ventromedial region of the RVLM. cGMP-IR in the neurons of the NA and in blood vessels (arrows) is evident (panels **b**, **d**, **f**) however there is no labelling of neurons with cGMP in association with either the PNMT or nNOS cell groups. A single cGMP-IR neuron is visible (arrow head, panel **f**) in the C1 region of the SHR animal. Scale bar in Panel (**b**) = 200 μm for panels (**a**, **b**). Scale bars in panels (**d**) and (**f**) equal 100 μm for panels (**c**, **d**) and (**e**, **f**), respectively
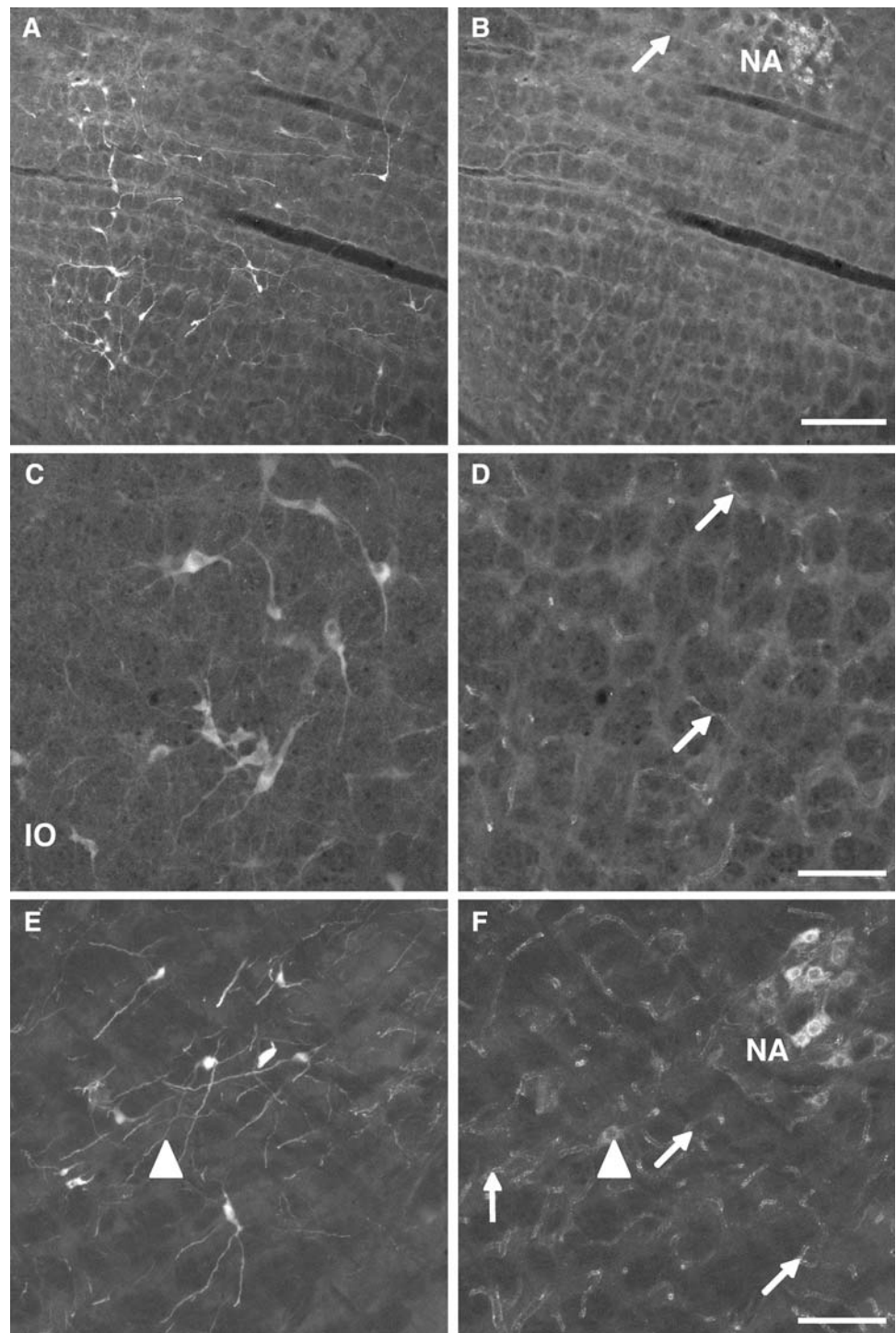
Detection of sGC-IR in the RVLM

In the fifth series of experiments, sections from WKY animals (10 weeks, $n = 3$) were examined for sGC/PNMT and sGC/nNOS-IR. Within the RVLM region, sGC-IR was widely distributed and unlike the PNMT and nNOS-IR neuronal populations, sGC cells did not localise to a distinct group or nuclei. Cells immunoreactive for sGC were often in close proximity to PNMT (Fig. 4a) or nNOS immunoreactive cells (data not shown) but there was no co-localisation.

The sixth and final series of experiments were undertaken in order to confirm the neuronal expression of sGC. Sections from WKY animals (10 weeks, $n = 3$) were double labelled for sGC and PGP-9.5 (neuronal specific marker). Parallel control experiments double labelling for
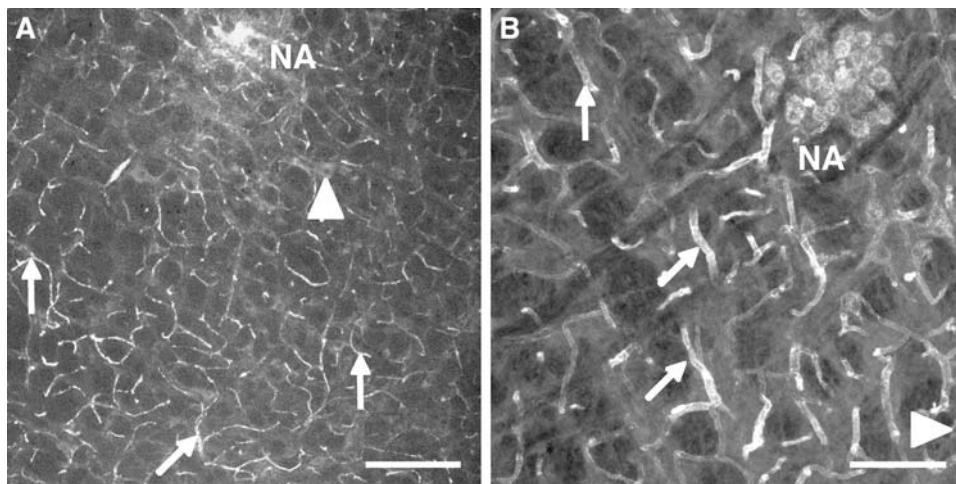
Fig. 2 Confocal images illustrating cGMP in RVLM sections taken from adult WKY (**a**) and SHR (**b**) animals treated with IBMX in the pre-perfusate solution. Midline is located to the left and ventral surface of the medulla towards the base. Figures show the marked increase in detection of cGMP in the vasculature (arrows) and cells of the NA when compared to Fig. 1, however very few neurons expressing cGMP were detected in the RVLM region. Individual neurons showing cGMP-IR above the level of background staining are shown (arrow heads). Scale bar in (**a**) equals 200 μm, scale bar in panel (**b**) equals 100 μm

sGC and a non-neuronal cell (astroglia: marker GFAP) were also performed. The cellular staining pattern for GFAP was consistent with the morphology and distribution of astroglia [40], and showed no colocalisation or pattern similarity to the sGC staining (Fig. 4b). In contrast, all cells showing sGC-IR were consistently double labelled with PGP9.5, confirming that sGC was expressed in neurones in the RVLM (Fig. 4c). Additional experiments in adult SHR ($n = 2$) showed the same expression pattern of sGC in PGP9.5-IR cells (data not shown).

Control experiments

Sections processed in the absence of primary antibody did not show any staining (Fig. 5a). Control experiments for sGC in the cerebellum showed the typical sGC-IR staining (Fig. 5b) as previously described by Ding et al [41]. Positive controls for PGP9.5 using a TH double label showed that all TH-IR neurons from the RVLM region also expressed PGP9.5-IR, in addition to adjacent neurons that expressed PGP9.5 only (Fig. 5c). Double labelling with alpha-SMA, which labels smooth muscle cells of precapillary arterioles in the brain [42], showed co-localisation with cGMP (Fig. 5d). Furthermore, our overall pattern of vascular/microvascular cGMP staining in the brain is as described by [31].

Discussion

It is well documented that the premotor sympathetic neurons in the RVLM are critical to the maintenance and control of blood pressure [43] and that endogenous NO is an important mediator in this regulatory process [9, 10, 21]. Functional studies provide strong evidence that NO acts through the sGC-cGMP signalling pathway in the RVLM to drive sympathoexcitatory responses [6, 20, 44, 45], however, we were unable to detect cGMP in the RVLM of either the SHR or WKY rat strains. This was despite the use of PDE inhibitors of the use of specific stimulators of cGMP synthesis in slice preparations. We were able to demonstrate abundant sGC-IR in neurones throughout the RVLM region.

Cyclic GMP in the RVLM

An inability to detect cGMP in the RVLM may have been associated with methodological issues, for example the adequacy of antigen recognition/penetration, or sensitivity of the technique. These concerns are alleviated somewhat by our detection of cGMP in the adjacent brainstem region of the NA. Alternative methodologies such as radioimmunoassay may have been more sensitive, however the ability to define specific neuronal populations is lost and in a study examining hippocampal slices, analysis of cGMP radioimmunoassay versus cGMP immunofluorescence intensity showed comparable sensitivities [46]. The lack of detectable cGMP expression in neurons of the RVLM is in accord with a detailed study by De Vente et al. [22], who similarly observed cGMP in the NA and nucleus tractus solitarii (NTS) in the brain stem region, but do not comment on its expression in the RVLM, despite the use of invitro stimulation paradigms as applied in this study. In the work by De Vente et al., the importance of IBMX to reveal

Fig. 3 Confocal images depicting cGMP (**b**, **d**, **e**) and either PNMT (**a**, **c**) or nNOS-IR (**e**) in RVLM sections from WKY rats after treatment in-vitro to increase cGMP synthesis. Panels (**a**) and (**b**) show the PNMT/cGMP-IR, respectively under control incubation conditions. Panels (**c**) and (**d**) illustrate PNMT/cGMP-IR respectively after in-vitro incubation in NMDA (100 μm 2 min). Panels (**e** and **f**) show nNOS/cGMP-IR, respectively after incubation in DETA-NO (100 μm 15 min). Insets **b′**, **d′** and **f′** illustrate cGMP expression in the NA under control, NMDA and DETA-NO experimental conditions, respectively. All experiments were performed in the presence of 0.5 mM IBMX. Despite cGMP-IR in blood vessels (arrows) and NA being enhanced by the in-vitro treatments, they failed to reveal the presence of additional cGMP-IR neurons in the RVLM regions in association with either the PNMT or nNOS cell groups. Scale bar in (**f**) equals 100 μm for panels (**a–f**). Scale bar in **f′** equals 100 μm for panels (**b′**, **d′** and **f′**)
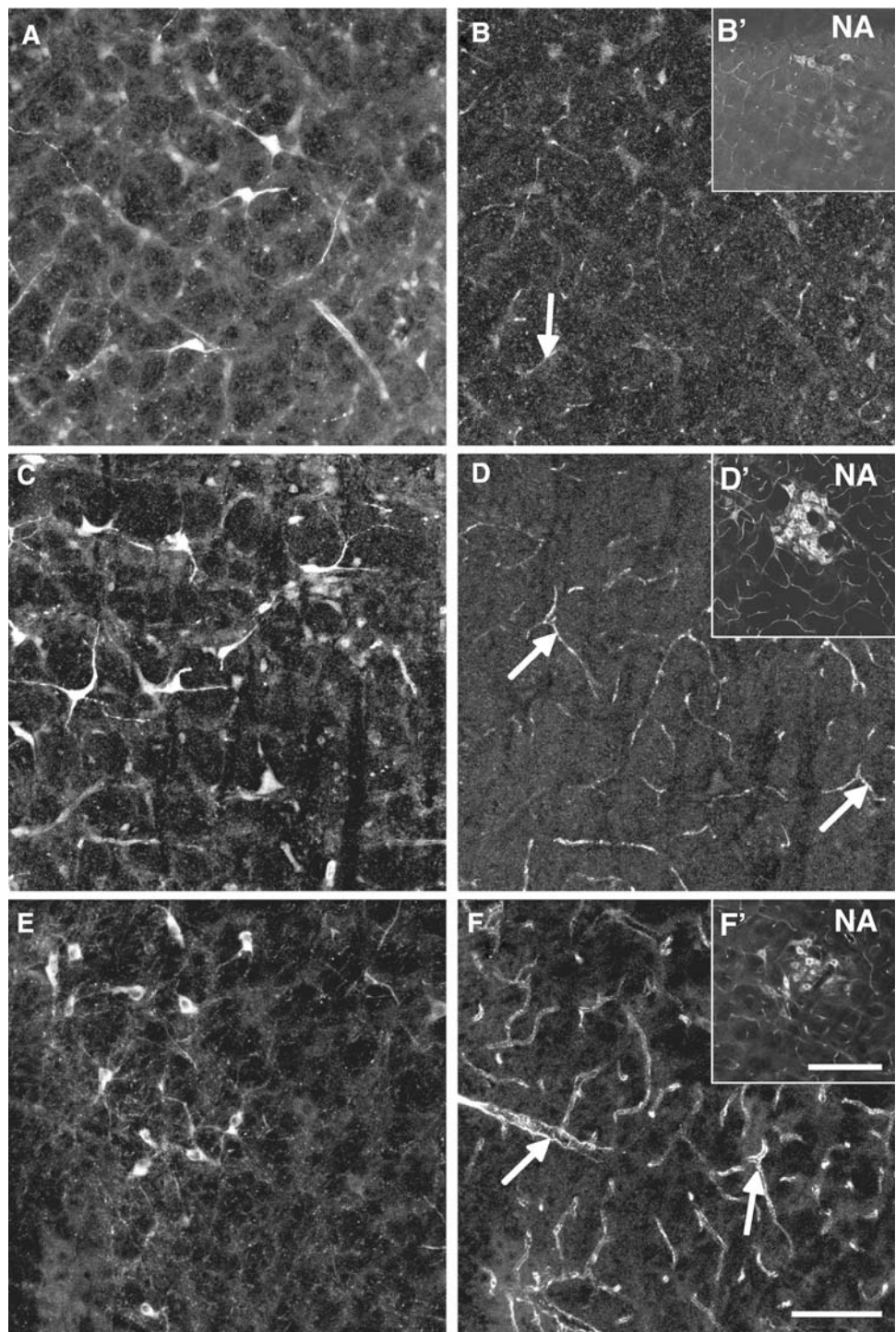
otherwise non-detectable cGMP populations was stressed [22, 47] and this has also been noted by other authors [48]. For this reason, IBMX was used in a subset of studies in perfusion fixed rats and for the brainstem slice in-vitro incubation experiments. However, while we found that IBMX did increase the levels of cGMP in already visible cell populations and in the vasculature of the brainstem, it did not uncover cGMP-IR neurons in the RVLM, suggesting IBMX-sensitive PDE activity did not limit detection. This concurs with our previous work examining cGMP levels in the spinal cord, where we were able to show that cGMP expressing sympathetic preganglionic neurons could be readily detected in the absence of IBMX [30]. The effects of anaesthetic on cGMP levels also require consideration. For this project, anaesthetic was an ethical requirement. Results from studies investigating the

Fig. 4 Confocal images illustrating double labelling for PNMT/sGC ▶ (**a**), GFAP/sGC (**b**) and PGP9.5/sGC (**c**) immunoreactivity in the RVLM from a WKY animal (male, 10-weeks-old). Panel (**a**) shows PNMT (red—CY3 secondary antibody) and sGC (green—FITC secondary antibody) double labelling and illustrates numerous cells IR for sGC (arrows) but lack of co localisation with PNMT (#). Panel (**b**) shows GFAP (red—CY3 secondary antibody) and sGC (green—FITC secondary antibody) and serves to demonstrate that the cells immunoreactive for sGC (arrows) show none of the characteristic morphological features of astrocytes (*) and that there is no double labelling for the two markers. Panel (**c**) shows PGP9.5 (red—CY3 secondary antibody) and sGC (green—FITC secondary antibody) and illustrates double labelling for all sGC cells (arrows; yellow), with adjacent neurons immunoreactive for PGP9.5 only (*). Scale bar in (**a**) equal 100 μm, scale bar in panels (**b**) and (**c**) equals 50 μm
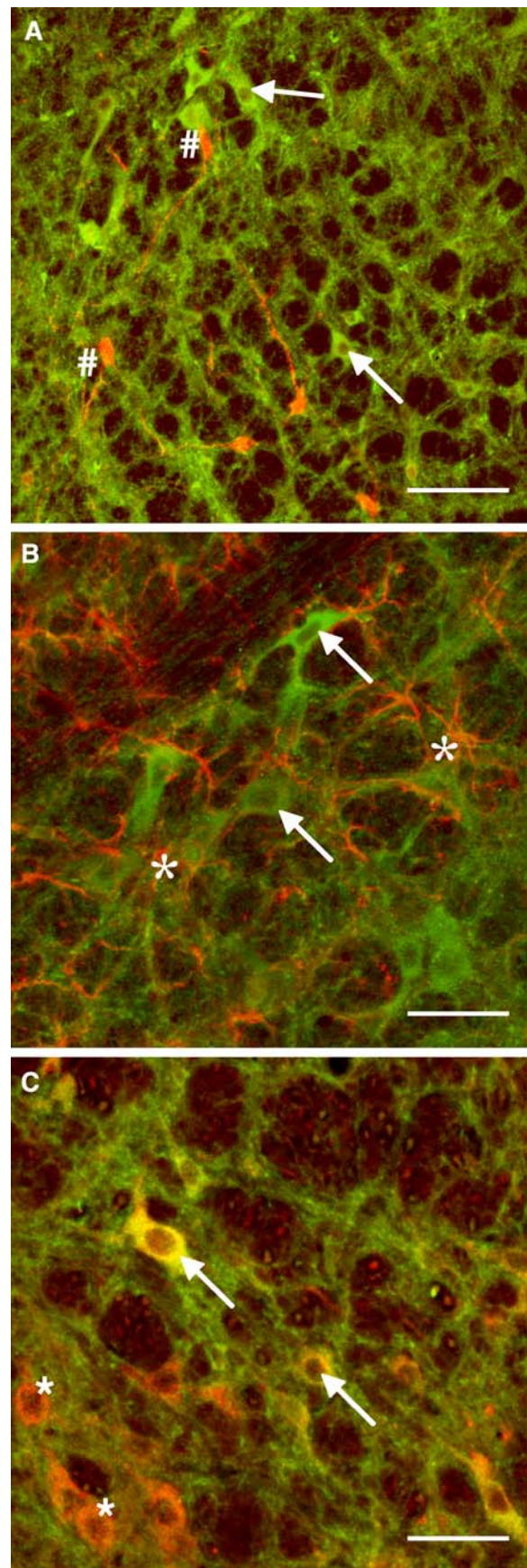
effect of anaesthetic on cGMP in the central nervous system are conflicting, with some reports describing the effects of anaesthetics as inhibitory, while others suggest no effect or indeed an increase in cGMP levels [49]. Thiopentone was chosen for this study on the rationale that intravenous agents are less likely to depress cGMP levels than inhalation anaesthetics [50], and that pentobarbital drugs specifically do not depress cGMP levels in the brainstem [51]. Given the time period available for anaesthetic washout and the demonstration of an increase of detectable cGMP in surrounding tissues, it is likely the effects of anaesthetic were minimal in this study.

The use of NMDA and NO donors to increase detectable cGMP in brain slice in-vitro preparations has been demonstrated previously in various tissues including the paraventricular nucleus [52] cerebellum [22, 47] and hippocampus and thalamus [46]. The choice of DETA-NO as a donor was based on its ability to spontaneously liberate NO in aqueous solutions in a stable, time-controlled fashion [53]. It has been proposed that the type of NO donor can make a significant difference to the way in which cGMP is stimulated [54], however a recent study comparing the effects of NONOates to the classical NO donor sodium nitroprusside found limited difference in their ability to stimulate sGC or influence cGMP staining patterns in brain slice preparations [46]. The NO donor nitroglycerin has also been shown to increase cGMP-IR in both neuronal and vascular elements of the brain, but in agreement with our study, did not uncover any additional or previously undetected cGMP immunoreactive neuronal cell groups [31].

Soluble guanylate cyclase expression within the RVLM

The widespread detection of sGC within neurones of the RVLM is in accord with previous studies that have demonstrated both mRNA and protein for sGC within the medulla [55, 56]. It is likely to be a functional form of sGC, as the antibody we used was specific for the β1 subunit, which is the obligatory subunit for functional sGC [15],
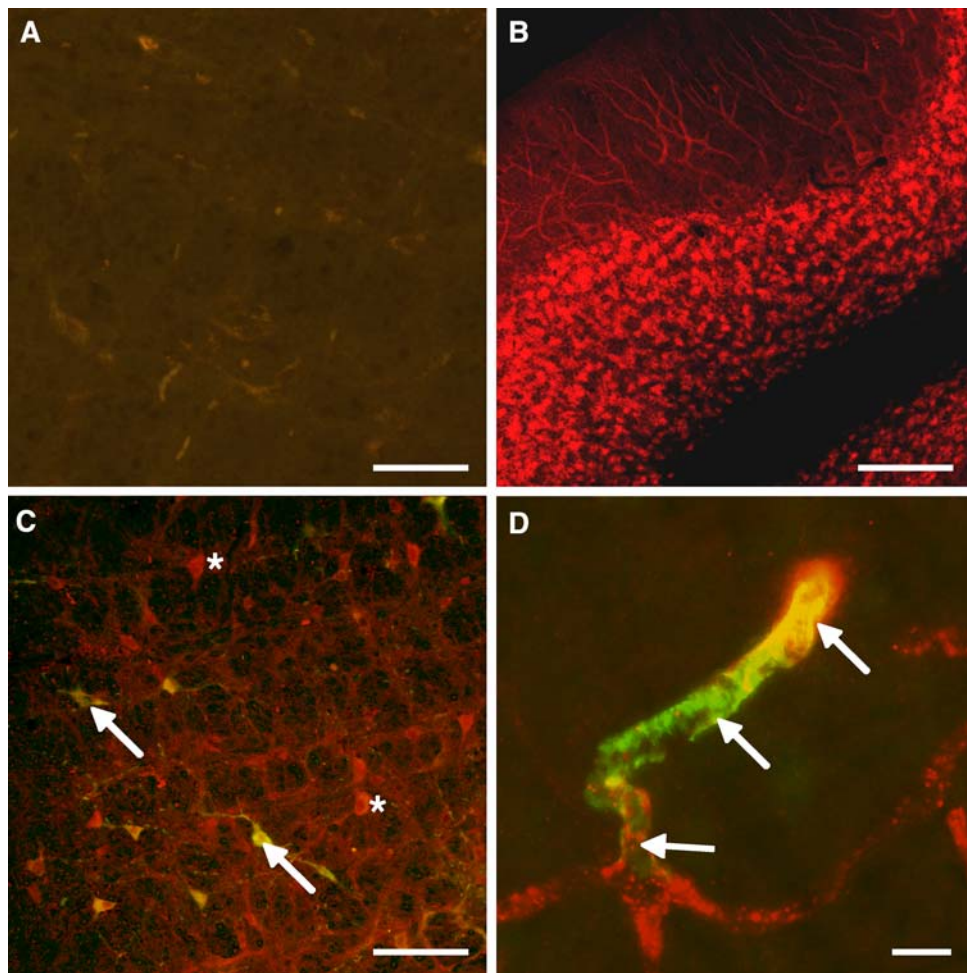
Fig. 5 Control experimental results. Panel (**a**) shows a negative control for PGP9.5 (red—CY3 secondary antibody) and sGC (green—FITC secondary antibody). Double labelling on a control RVLM section from a 10-week-old WKY shows no immunoreactivity for either series of labelling reactions. Panel (**b**) shows intense labelling for sGC (red—CY3 secondary antibody) in the cerebellum from a 10 week old WKY. Panel (**c**) shows positive control experiments for PGP9.5 from an adult SHR animal. All TH positive cells (green—FITC secondary antibody) were double labelled for PGP9.5 (red—CY3 secondary antibody) resulting in a yellow colour on the overlaid images (arrows). Immediately adjacent to the double-labelled cells are PGP9.5 only labelled neurons (*). Panel (**d**) shows control experiments assessing the vascular expression of cGMP in a 10 week old WKY. Sections were double labelled for alpha-smooth muscle actin (alpha-SMA; green—FITC secondary antibody) and cGMP (red—CY3 antibody). All alpha-SMA-IR structures showed clear co-localisation with cGMP as illustrated. The cGMP expression can be seen to extend from the larger precapillary arteriole (arrows) to the microvasculature, where it is expressed in pericytes (the contractile elements of the brain microvasculature) that do not label for alpha-SMA [64, 65]. Scale bar in (**a**) equal 50 μm, scale bar in panels (**b**) and (**c**) equal 100 μm, scale bar in panel (**d**) equals 20 μm

and has been shown to co-localise extensively with the α subunit throughout the CNS of the adult rat brain [41].

While we did not demonstrate co-localisation of sGC with the nNOS cell population, they were often in close association. This pattern of expression is consistent with other brain regions, where NO responsive and NO producing structures are not found within the same neuronal profile [22, 41, 57]. An exception is the NTS, where nNOS and sGC have been shown to co-localise [58]. Similarly, we saw sGC in close association but not co-localised with the C1 cell group. Additional studies aimed at determining the cell population which expresses sGC should include retrograde labelling as a means of identification of the non-

C1 bulbospinal group [2], and double labelling for markers such as neuropeptide Y to identify neurons which project to the hypothalamus [59], or markers to enable identification of glutamatergic and gabaergic neurons [3]. This would then allow potential functional relevance to be attributed to sGC expression in the region.

Conclusion

A number of physiological studies indicate that NO can modulate pressor and reflex responses in the RVLM via an sGC/cGMP dependent mechanism [6, 7, 44, 45]. While we

were unable to detect cGMP-IR in the neurons of the C1 region, either in the resting state, when stimulated by NMDA or NO donor, or after PDE inhibition, our sGC-IR results certainly indicate the capacity for cGMP synthesis. In an in-vivo study of the cat, nNOS-sGC co-localisation was present in the RVLM only after activation by bradycardia (as identified by the presence of *c-fos*) [60]. This raises the hypothesis that functional network inputs, such as the sympathetic baroreflex pathway [45] are required to drive a sGC/cGMP cascade in the RVLM. This may be the mechanism by which functional differences in the SHR and WKY are delineated and future studies investigating this possibility are warranted.

Basal cGMP levels in neurons are the result of a dynamic equilibrium between synthesis, driven by NO-sGC, and the rate of degradation by PDEs, [61]. The rate of synthesis can change with time due to desensitisation of sGC, and cGMP kinetics can vary between not only different cell types but also different regions of the brain [62]. The expression of IBMX-insensitive PDEs, such as PDE9, which is specific for cGMP [46, 63], may be another important factor limiting detection of cGMP accumulation in regions such as the RVLM. Of note is a recent study that has shown under similar conditions to ours, that the use of an NO donor in the presence of IBMX was not sufficient to maximise cGMP detection in the hippocampus, but instead required the further addition of the NO-independent activators of sGC: YC-1 or BAY 41-2272 [46]. This stimulated cGMP synthesis in cells not normally known to express cGMP and the authors suggest the presence of an endogenous sGC inhibitor as a possible explanation [46]. Examination of the role of functional stimulatory inputs, NO-independent activation of sGC and the activity of specific PDEs is therefore required before the definitive role of cGMP as a contributor to altered sympathetic tone in the SHR can be ascertained.

References

1. Lipski J, Kanjhan R, Kruszewska B, Smith M (1995) Barosensitive neurons in the rostral ventrolateral medulla of the rat in vivo: morphological properties and relationship to C1 adrenergic neurons. Neuroscience 69:601–618

2. Phillips JK, Goodchild AK, Dubey R, Sesiashvili E, Takeda M, Chalmers J, Pilowsky PM, Lipski J (2001) Differential expression of catecholamine biosynthetic enzymes in the rat ventrolateral medulla. J Comp Neurol 432(1):20–34

3. Stornetta RL, Sevigny CP, Schreihofer AM, Rosin DL, Guyenet PG (2002) Vesicular glutamate transporter DNPI/VGLUT2 is expressed by both C1 adrenergic and nonaminergic presympathetic vasomotor neurons of the rat medulla. J Comp Neurol 444(3):207–220

4. Sved AF, Ito S, Madden CJ, Stocker SD, Yajima Y (2001) Excitatory inputs to the RVLM in the context of the baroreceptor reflex. Ann N Y Acad Sci 940:247–258

5. Chen SY, Mao SP, Chai CY (2001) Role of nitric oxide on pressor mechanisms within the dorsomedial and rostral ventrolateral medulla in anaesthetized cats. Clin Exp Pharmacol Physiol 28(3):155–163

6. Wu WC, Wang Y, Su CK, Chai CY (2001) The nNOS/cGMP signal transducing system is involved in the cardiovascular responses induced by activation of NMDA receptors in the rostral ventrolateral medulla of cats. Neurosci Lett 310(2–3):121–124

7. Huang CC, Chan SH, Hsu K (2003) cGMP/protein kinase G-dependent potentiation of glutamatergic transmission induced by nitric oxide in immature rat rostral ventrolateral medulla neurons in vitro. Mol Pharmacol 64(2):521–532

8. Krukoff TL (1998) Central regulation of autonomic function: no brakes? Clin Exp Pharmacol Physiol 25(6):474–478

9. Hirooka Y, Polson JW, Dampney RA (1996) Pressor and sympathoexcitatory effects of nitric oxide in the rostral ventrolateral medulla. J Hypertens 14(11):1317–1324

10. Martins-Pinge MC, Baraldi-Passy I, Lopes OU (1997) Excitatory effects of nitric oxide within the rostral ventrolateral medulla of freely moving rats. Hypertension 30(3 Pt 2):704–707

11. Tseng CJ, Liu HY, Lin HC, Ger LP, Tung CS, Yen MH (1996) Cardiovascular effects of nitric oxide in the brain stem nuclei of rats. Hypertension 27(1):36–42

12. Ahern GP, Klyachko VA, Jackson MB (2002) cGMP and *S*-nitrosylation: two routes for modulation of neuronal excitability by NO. Trends Neurosci 25(10):510–517

13. Lucas KA, Pitari GM, Kazerounian S, Ruiz-Stewart I, Park J, Schulz S, Chepenik KP, Waldman SA (2000) Guanylyl cyclases and signaling by cyclic GMP. Pharmacol Rev 52(3):375–414

14. Mergia E, Russwurm M, Zoidl G, Koesling D (2003) Major occurrence of the new alpha2beta1 isoform of NO-sensitive guanylyl cyclase in brain. Cell Signal 15(2):189–195

15. Friebe A, Mergia E, Dangel O, Lange A, Koesling D (2007) Fatal gastrointestinal obstruction and hypertension in mice lacking nitric oxide-sensitive guanylyl cyclase. Proc Natl Acad Sci USA 104(18):7699–7704

16. Ohkuma S, Katsura M (2001) Nitric oxide and peroxynitrite as factors to stimulate neurotransmitter release in the CNS. Prog Neurobiol 64(1):97–108

17. Chang AY, Chan JY, Chan SH (2003) Differential distribution of nitric oxide synthase isoforms in the rostral ventrolateral medulla of the rat. J Biomed Sci 10(3):285–291

18. Edwards MA, Loxley RA, Powers-Martin K, Lipski J, McKitrick DJ, Arnolda LF, Phillips JK (2004) Unique Levels of Expression of *N*-methyl-D-aspartate receptor subunits and neuronal nitric oxide synthase in the rostral ventrolateral medulla of the spontaneously hypertensive rat. Mol Brain Res 129:33–43

19. Chan SH, Wang LL, Chan JY (2003) Differential engagements of glutamate and GABA receptors in cardiovascular actions of endogenous nNOS or iNOS at rostral ventrolateral medulla of rats. Br J Pharmacol 138(4):584–593

20. Chan JY, Chan SH, Li FC, Tsai CY, Cheng HL, Chang AY (2005) Phasic cardiovascular responses to mevinphos are mediated through differential activation of cGMP/PKG cascade and peroxynitrite via nitric oxide generated in the rat rostral ventrolateral medulla by NOS I and II isoforms. Neuropharmacology 48(1):161–172

21. Morimoto S, Sasaki S, Miki S, Kawa T, Nakamura K, Itoh H, Nakata T, Takeda K, Nakagawa M, Fushiki S (2000) Nitric oxide

is an excitatory modulator in the rostral ventrolateral medulla in rats. Am J Hypertens 13(10):1125–1134

22. De Vente J, Hopkins DA, Markerink-Van Ittersum M, Emson PC, Schmidt HH, Steinbusch HW (1998) Distribution of nitric oxide synthase and nitric oxide-receptive, cyclic GMP-producing structures in the rat brain. Neuroscience 87(1):207–241

23. Iadecola C, Faris PL, Hartman BK, Xu X (1993) Localization of NADPH diaphorase in neurons of the rostral ventral medulla: possible role of nitric oxide in central autonomic regulation and oxygen chemoreception. Brain Res 603(1):173–179

24. Tsuchihashi T, Kagiyama S, Matsumura K, Lin Y, Abe I, Fujishima M (2000) Cardiovascular responses to glutamate and angiotensin II in ventrolateral medulla of hypertension induced by chronic inhibition of nitric oxide. Hypertens Res 23(4):359–364

25. Tsuchihashi T, Kagiyama S, Ohya Y, Abe I, Fujishima M (1998) Antihypertensive treatment and the responsiveness to glutamate in ventrolateral medulla. Hypertension 31(1):73–76

26. Moyer JR Jr, Brown TH (1998) Methods for whole-cell recording from visually preselected neurons of perirhinal cortex in brain slices from young and aging rats. J Neurosci Methods 86(1):35–54

27. Lerma J, Kushner L, Zukin RS, Bennett MV (1989) N-methyl-D-aspartate activates different channels than do kainate and quisqualate. Proc Natl Acad Sci USA 86(6):2083–2087

28. Sandirasegarane L, Diamond J (1999) The nitric oxide donors, SNAP and DEA/NO, exert a negative inotropic effect in rat cardiomyocytes which is independent of cyclic GMP elevation. J Mol Cell Cardiol 31(4):799–808

29. Paxinos G, Carrive P, Wang H, Wang PU (eds) (1999) Chemoarchitectonic atlas of the rat brainstem. Academic Press, San Diego

30. Powers-Martin K, McKitrick DJ, Arnolda LF, Phillips JK (2006) Distinct subpopulations of cyclic guanosine monophosphate (cGMP) and neuronal nitric oxide synthase (nNOS) containing sympathetic preganglionic neurons in spontaneously hypertensive and Wistar–Kyoto rats. J Comp Neurol 497(4):566–574

31. Tassorelli C, Blandini F, Greco R, Nappi G (2004) Nitroglycerin enhances cGMP expression in specific neuronal and cerebrovascular structures of the rat brain. J Chem Neuroanat 27(1):23–32

32. Dinerman JL, Dawson TM, Schell MJ, Snowman A, Snyder SH (1994) Endothelial nitric oxide synthase localized to hippocampal pyramidal cells: implications for synaptic plasticity. Proc Natl Acad Sci USA 91(10):4214–4218

33. Gutierrez-Mecinas M, Crespo C, Blasco-Ibanez JM, Gracia-Llanes FJ, Marques-Mari AI, Martinez-Guijarro FJ (2005) Soluble guanylyl cyclase appears in a specific subset of periglomerular cells in the olfactory bulb. Eur J Neurosci 21(5):1443–1448

34. Rinaman L (2001) Postnatal development of catecholamine inputs to the paraventricular nucleus of the hypothalamus in rats. J Comp Neurol 438(4):411–422

35. Chu Y, Kompoliti K, Cochran EJ, Mufson EJ, Kordower JH (2002) Age-related decreases in Nurr1 immunoreactivity in the human substantia nigra. J Comp Neurol 450(3):203–214

36. Trowern AR, Laight R, MacLean N, Mann DA (1996) Detection of neuron-specific protein gene product (PGP) 9.5 in the rat and zebrafish using anti-human PGP9.5 antibodies. Neurosci Lett 210(1):21–24

37. Alvarado LT, Perry GM, Hargreaves KM, Henry MA (2007) TRPM8 Axonal expression is decreased in painful human teeth with irreversible pulpitis and cold hyperalgesia. J Endod 33(10):1167–1171

38. Debus E, Weber K, Osborn M (1983) Monoclonal antibodies specific for glial fibrillary acidic (GFA) protein and for each of the neurofilament triplet polypeptides. Differentiation 25(2):193–203

39. Skalli O, Ropraz P, Trzeciak A, Benzonana G, Gillessen D, Gabbiani G (1986) A monoclonal antibody against alpha-smooth muscle actin: a new probe for smooth muscle differentiation. J Cell Biol 103(6 Pt 2):2787–2796

40. Lyck L, Jelsing J, Jensen PS, Lambertsen KL, Pakkenberg B, Finsen B (2006) Immunohistochemical visualization of neurons and specific glial cells for stereological application in the porcine neocortex. J Neurosci Methods 152(1–2):229–242

41. Ding JD, Burette A, Nedvetsky PI, Schmidt HH, Weinberg RJ (2004) Distribution of soluble guanylyl cyclase in the rat brain. J Comp Neurol 472(4):437–448

42. Boado RJ, Pardridge WM (1994) Differential expression of alpha-actin mRNA and immunoreactive protein in brain microvascular pericytes and smooth muscle cells. J Neurosci Res 39(4):430–435

43. Dampney RA (1994) Functional organization of central pathways regulating the cardiovascular system. Physiol Rev 74(2):323–364

44. Martins-Pinge MC, Araujo GC, Lopes OU (1999) Nitric oxide-dependent guanylyl cyclase participates in the glutamatergic neurotransmission within the rostral ventrolateral medulla of awake rats. Hypertension 34(4 Pt 2):748–751

45. Mayorov DN (2005) Selective sensitization by nitric oxide of sympathetic baroreflex in rostral ventrolateral medulla of conscious rabbits. Hypertension 45(5):901–906

46. van Staveren WC, Markerink-van Ittersum M, Steinbusch HW, Behrends S, de Vente J (2005) Localization and characterization of cGMP-immunoreactive structures in rat brain slices after NO-dependent and NO-independent stimulation of soluble guanylyl cyclase. Brain Res 1036(1–2):77–89

47. De Vente J, Bol JG, Berkelmans HS, Schipper J, Steinbusch HM (1990) Immunocytochemistry of cGMP in the cerebellum of the immature, adult, and aged rat: the involvement of nitric oxide. A micropharmacological study. Eur J Neurosci 2(10):845–862

48. Allaerts W, De Vente J, Markerink-Van Ittersum M, Tuinhof R, Roubos EW (1998) Topographical relationship between neuronal nitric oxide synthase immunoreactivity and cyclic 3′, 5′-guanosine monophosphate accumulation in the brain of the adult Xenopus laevis. J Chem Neuroanat 15(1):41–56

49. Galley HF (2000) Anaesthesia and the nitric oxide-cyclic GMP pathway in the central nervous system. Br J Anaesth 84(2):141–143

50. Tobin JR, Martin LD, Breslow MJ, Traystman RJ (1994) Selective anesthetic inhibition of brain nitric oxide synthase. Anesthesiology 81(5):1264–1269

51. Galley HF, Le Cras AE, Logan SD, Webster NR (2001) Differential nitric oxide synthase activity, cofactor availability and cGMP accumulation in the central nervous system during anaesthesia. Br J Anaesth 86(3):388–394

52. Vacher CM, Hardin-Pouzet H, Steinbusch HW, Calas A, De Vente J (2003) The effects of nitric oxide on magnocellular neurons could involve multiple indirect cyclic GMP-dependent pathways. Eur J Neurosci 17(3):455–466

53. Keefer LK (2005) Nitric oxide (NO)- and nitroxyl (HNO)-generating diazeniumdiolates (NONOates): emerging commercial opportunities. Curr Top Med Chem 5(7):625–636

54. Butt E, Pohler D, Genieser HG, Huggins JP, Bucher B (1995) Inhibition of cyclic GMP-dependent protein kinase-mediated effects by (Rp)-8-bromo-PET-cyclic GMPS. Br J Pharmacol 116(8):3110–3116

55. Campese VM, Sindhu RK, Ye S, Bai Y, Vaziri ND, Jabbari B (2007) Regional expression of NO synthase, NAD(P)H oxidase and superoxide dismutase in the rat brain. Brain Res 1134(1):27–32

56. Krukoff TL, Gehlen F, Ganten D, Wagner J (1995) Gene expression of brain nitric oxide synthase and soluble guanylyl

cyclase in hypothalamus and medulla of two kidney, one clip hypertensive rats. Hypertension 26:171–176

57. Schmidt HH, Gagne GD, Nakane M, Pollock JS, Miller MF, Murad F (1992) Mapping of neural nitric oxide synthase in the rat suggests frequent co-localization with NADPH diaphorase but not with soluble guanylyl cyclase, and novel paraneural functions for nitrinergic signal transduction. J Histochem Cytochem 40(10):1439–1456

58. Lin LH, Talman WT (2005) Soluble guanylate cyclase and neuronal nitric oxide synthase colocalize in rat nucleus tractus solitarii. J Chem Neuroanat 29(2):127–136

59. Verberne AJM, Stornetta RL, Guyenet PG (1999) Properties of C1 and other ventrolateral medullary neurones with hypothalamic projections in the rat. J Physiol 517(2):477–494

60. Guo ZL, Longhurst JC (2006) Responses of neurons containing VGLUT3/nNOS-cGMP in the rVLM to cardiac stimulation. Neuroreport 17(3):255–259

61. Hepp R, Tricoire L, Hu E, Gervasi N, Paupardin-Tritsch D, Lambolez B, Vincent P (2007) Phosphodiesterase type 2 and the homeostasis of cyclic GMP in living thalamic neurons. J Neurochem 102(6):1875–1886

62. Mo E, Amin H, Bianco IH, Garthwaite J (2004) Kinetics of a cellular nitric oxide/cGMP/phosphodiesterase-5 pathway. J Biol Chem 279(25):26149–26158

63. Soderling SH, Bayuga SJ, Beavo JA (1998) Identification and characterization of a novel family of cyclic nucleotide phosphodiesterases. J Biol Chem 273(25):15553–15558

64. Ehler E, Karlhuber G, Bauer HC, Draeger A (1995) Heterogeneity of smooth muscle-associated proteins in mammalian brain microvasculature. Cell Tissue Res 279(2):393–403

65. Poeggel G, Muller M, Seidel I, Rechardt L, Bernstein HG (1992) Histochemistry of guanylate cyclase, phosphodiesterase, and NADPH-diaphorase (nitric oxide synthase) in rat brain vasculature. J Cardiovasc Pharmacol 20(Suppl 12):S76–S79